SimBuild
2024

Eleventh National Conference of IBPSA-USA
Denver, Colorado
May 21 – 23, 2024

Building-Grid Interaction Analysis of an All-Electric Office Building with Thermally Activated Building Systems Using Rule Based Control and Dynamic Tariff Signals

Tuğçin Kırant-Mitić[1], Karsten Voss[1]
University of Wuppertal, Wuppertal, Germany

Abstract

The integration of renewable energy sources into power grids leads to increased instability due to their inherent intermittency (Li and Wang et al. 2020). These challenges necessitate the development of effective strategies (Li and Satchwell et al. 2022). Collaboration between building systems and the power grid, known as building-grid interaction, emerges as a promising solution to mitigate these challenges. This research examines building-grid interaction with a focus on an all-electric office building with thermally activated ceilings. A rule-based control algorithm is embedded within the simulation environment. The results demonstrate that such collaborative systems can significantly enhance grid stability while optimizing building energy performance.

Introduction

Thermally Activated Building Systems (TABS) embed heating and cooling elements within the building structure, harnessing building envelope as thermal reservoirs (Arteconi and Costola et al. 2014). In recent years, TABS have garnered growing favor due to their capacity to deliver enhanced thermal comfort and heightened energy efficiency (Chen, Li and Feng 2021) making use of environmental heat sources and sinks. Building elements, such as ceilings and floor slabs, function as thermal energy storage, leveraging their dynamic thermal behavior to facilitate space heating/cooling by releasing stored energy (Lehmann, Dorer and Koschenz 2007). TABS contribute to energy efficiency by allowing slightly lower heating setpoints and higher cooling setpoints while maintaining comfort (Rhee and Kim 2015; Salt 1985).

The literature categorizes various types of TABS -based on their intended operation mode, position, and working fluid- named such as radiant floor, radiant ceiling, hollow core slab, concrete core slab and pipe-embedded envelopes (Romaní, Gracia and Cabeza 2016). Compared to well established air-based HVAC systems, the implementation of control measures in TABS poses new challenges (Feng and Chuang et al. 2015). Since this system is characterized by water pipes embedded in building structure, exhibit a sluggish response to control signals attributable to their substantial thermal inertia. This constraint hinders the control system's ability to quickly address sudden thermal load changes leading to increased energy consumption from frequent mode switches (Tian and Love 2009).

TABS are typically regulated controlling supply water temperature and flow rate (Gwerder and Lehmann et al. 2008, Rhee, Olesen and Kim 2017). The heating/cooling curve adjusts the supply water temperature based on outdoor air temperature, and water flow rate to individual zones aligns with indoor set point temperatures (Lim and Jo et al. 2006, B.W. Olesen 2007). Some research suggest slab or floor surface temperatures can be used for control (Shin and Rhee et al. 2015, Cho and Zaheer-uddin 1999). Furthermore, there are theoretical frameworks that focus on estimating the state of charge by analyzing the temperature differential (delta T). In this case, meticulous installation of a surface temperature sensor is essential (Vivek and Rakesh et al. 2023). In Romaní, Gracia and Cabeza (2016), more information of TABS control strategies are given. In addition to the diverse manipulation variables, the operation mode, either continuous or intermittent, can also be implemented (Cho and Zaheer-uddin 1999). In continuous mode, the system is continuously monitored and controlled by thermostat feedback. Conversely, in the latter case, the operation is implemented where the system is active during specific hours throughout the day.

The integration of TABS with renewable energy sources and heat pumps can effectively reduce reliance on primary energy sources, enhances overall energy efficiency and consequently leading to a subsequent decrease in operational costs (Chen, Li and Feng 2021). In these hydronic systems, thermal energy is mostly extracted from the ground as resource to be utilized by a heat pump (Self et al. 2013) and is then distributed to the building structure via embodied piping to charge the envelope. However, this underscores the necessity for the development of more sophisticated building control strategies to effectively harness the potential synergy between hydronic systems, renewable energy sources, and the building envelope for optimal energy management.

In traditional energy systems, the electricity demand in a building is typically met by the centralized utility grid. This supply is usually stable and can be adjusted to meet fluctuations in demand. However, distributed energy systems as part of the power grids often generate energy intermittently (Li and Wang et al. 2020). This can lead to a mismatch between when energy is generated and when it is needed within the building. The energy demand and supply mismatch can have several implications such as affecting the stability of the power grid if not managed effectively. Buildings play a pivotal role in bolstering the stability of power grids, and it is important to acknowledge that the potential for building-grid interaction (Balaras 1996) is dependent on the availability of thermal mass within the building structure.

To address this challenge, innovative building control approaches have been developed Li and Satchwell et al. 2022). These approaches consider the building's thermal characteristics, HVAC system, and dynamic grid pricing or CO_2-factors. They leverage the building envelope as a structural thermal storage medium, offering a pathway to harness building-grid interaction potential. This ensures that energy demand aligns with periods of lower cost and availability (Reynders, Nuytten and Saelens 2013).

Focusing on an all-electric office building with concrete core activation in Niederanven, Luxembourg, this research provides insights into optimizing energy performance through thermally activated ceilings—a topic that, to date, has not been extensively explored. By actively exploiting the building's thermal storage capacity, this paper seeks to align heating demands with the power market, thus contributing new insights to the field of building-grid interaction.

In this study, we have conducted building energy simulations for a nearly zero-energy office building using rule-based control strategies. By leveraging the price signal from the Germany-Luxembourg bidding zone, we optimize the activation of the building's thermal storage capabilities in the heating season. The findings include comprehensive analyses of surface temperature variations and heat flux across office zones located at each corner of the building (South-East, North-West, South-West, North-East), as well as evaluations of indoor operative temperatures. This data is synthesized to elucidate the intricacies of building-grid interaction. The investigation emphasizes key performance indicators such as shifted electrical energy demand, altered electrical consumption from the power grid, and resultant cost variations, providing insights into the economic and operational efficiencies achieved through this interactive approach.

The case study building

The case study building (Figure 1), with an energy reference area of 2,600 m^2, is situated in Niederanven, Luxembourg (Lichtmess 2018). This region is characterized by an annual average temperature of 11°C and a global horizontal radiation of 150W/m^2 (Stackhouse 2023), representative of typical climate conditions in Central Europe.

Figure 1 The view of the case building Andy Staff (2022)

It is designed to utilize its concrete ceilings as a dual conduit for thermal energy transfer and air distribution. The building's heating and cooling demands are met by a geothermal borehole setup consisting of a heat pump system, which draws energy from a field of 21 geothermal probes, each extending to a depth of 100 meters, and offering a total heating capacity of 57 kW and a Coefficient of Performance (COP) of 4. Ground temperature fluctuations are more pronounced at depths shallower than 0.8 m, decreasing with greater depth (Hanova and Dowlatabadi 2007). Ground source heat pumps harness the stable ground temperature, warmer than the winter air and cooler than the summer air (Lee 2011). The building fulfills its cooling requirements passively by harnessing a geothermal probe field with a capacity of 74 kW, along with the implementation of automated nighttime window ventilation for enhanced natural temperature regulation. In periods of prolonged cooling demand, the heat pump system is dual-purposed to provide cooling, with a capacity of 45 kW, effectively employing the ground or the probe field as an energy-efficient recooler to sustain comfortable indoor temperatures. Figure 2 illustrates the comprehensive HVAC system of the case building, detailing the interplay between various system components and their interactions with electrical and environmental energy sources.

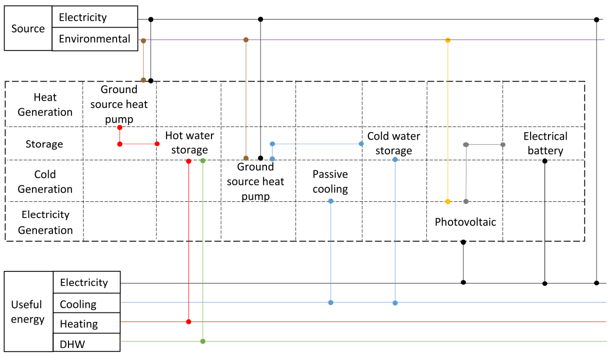

Figure 2 Integration of HVAC system components with energy resources in the case building

The building design incorporates pipe coils in the lower zones of the concrete ceilings, mirroring the principle of underfloor heating. These coils circulate water, subtly adjusting the ceiling temperature to 24°C for heating purposes or reducing it to 18°C to cool the space during warmer months. Indoor air quality is actively managed by introducing fresh air through an air handling unit (AHU) with a substantial capacity of 11,000 m³/h, regulated by CO_2 levels to ensure a healthy indoor environment. The system boasts a heat recovery efficiency of 80%, with a specific fan power of 0.51 W/(m³/h), striking a balance between energy efficiency and air quality. In the pursuit of energy independence, the building's electrical demand is predominantly satisfied by a rooftop photovoltaic (PV) installation which of 35 kW_p. Complementing this, a battery storage system with a capacity of 20 kWh is employed to capitalize on the PV system's energy yield, storing excess power for use.

Simulation

The analysis presented in this paper was conducted using the dynamic building energy simulation software IDA Indoor Climate and Energy-version 4.8 (IDA-ICE 2023). To ensure accuracy, the simulation's energy profiles including heat pump, circulation pumps, AHU fans, PV, battery, lighting, and user-related loads were calibrated against historically monitored data supplied by the building owners. Following this calibration, a specialized energy model was developed within IDA-ICE to examine the building's operational flexibility (Figure 3).

In the baseline scenario, hereafter referred to as Business-as-usual (BAU), the TABS control is integrated as follows: The heat pump operation adjusts the flow temperature set-point according to a predefined heating curve, which responds to changes in ambient temperature. Concurrently, the system's control strategy includes feedback from indoor temperature sensors. Moreover, the concrete core temperature is continuously monitored to ensure that the operation stays within the specified thermal limits. The system employs a continuous operation mode in reaction to thermostat readings to minimize temperature oscillations within the space. Electricity generated by the PV system initially meets the building's electrical demand. Any surplus generation is then used to charge the battery. Notably, the battery does not receive charging from the power grid or any other external sources.

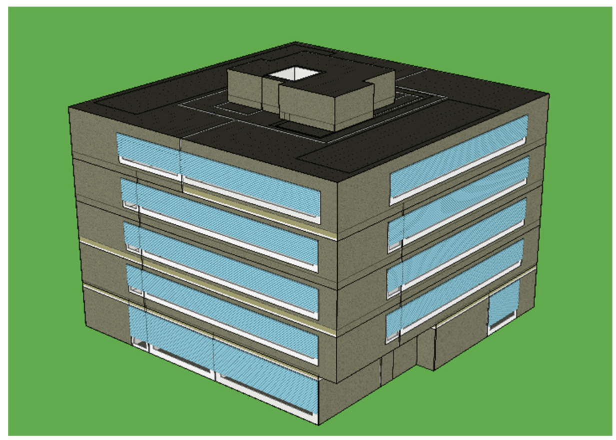

Figure 3 The energy model view of the case building

In Flexible Case (FC) analysis, specifically focuses on optimizing energy use during the heating period in this research, the building-grid interaction is examined using historical electricity spot prices (before tax) from the 2022 Luxembourg power grid data, which acts as a penalty signal to facilitate load optimization. A rule-based control algorithm is embedded in the simulation environment, enabling real-time optimization of the building's all energy consumption by controlling heat pump and battery at a 60-minute time step. The rule-based control algorithm is integrated to control macro in the simulation environment to respond to those signal levels. Figure 4 (A) illustrates the price data for a representative week of December 5th to December 11th used in the simulation, which is sourced from the ENTSO-E Transparency Platform (Dec-2022).

To conduct the analysis, the hourly price signal is grouped into 3 levels as cheap, normal, and expensive using 25% quartile analysis for each simulation day (Figure 4 (B)). During periods when electricity costs are at their lowest, as determined by the lower quartile of historical spot prices, the building's control system adjusts the setpoint temperature of the hot water tank, which has a capacity of 4500 liters, to be 2°C higher than the baseline setpoint defined in the BAU scenario (Figure 5).

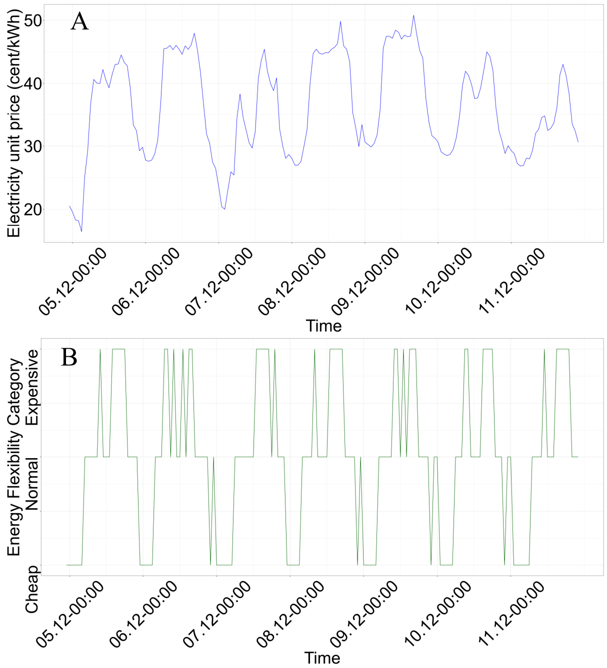

Figure 4 Electricity unit price (before tax) (A) and its categorization as a penalty signal for FC operation (B)

Simultaneously, it charges the battery until the State of Charge (SoC) reaches 100%. This likely corresponds to periods of increased temperature profiles in the FC scenarios, where energy is used more intensively to heat the building, taking advantage of the low prices.

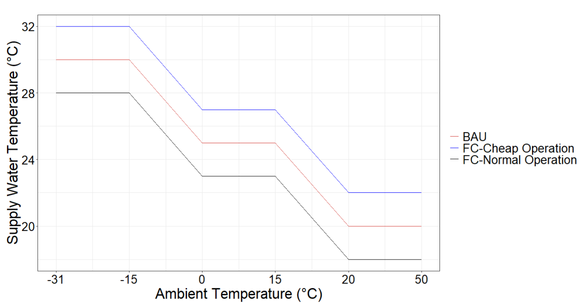

Figure 5 The heating curve based on the outdoor temperature

When prices are at normal levels, the control system decreases the setpoint temperature by 2 °C to avoid excessive energy use. Meanwhile, the system monitors the SoC of the battery; if it falls below 60%, the system initiates charging until the SoC reaches 60%. Conversely, if the SoC is higher, the system discharges the battery to meet the building's electrical demand.

During expensive electricity periods, the building minimizes its demand to reduce costs. This likely translates to the lower temperature readings during peak price hours by switching off the active heating system.

During these times, the building's electrical demand—excluding heating since the system is not running—is met by discharging the battery, provided sufficient charge is available. The operational control strategies are presented in Figure 6. In addition to these control strategies, a feed-in approach is applied when there is excess energy; this is included in the shifted cost calculation by applying the same electricity unit tariff as shown in Figure 4.

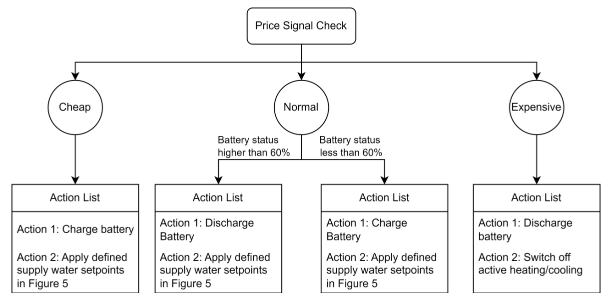

Figure 6 Building control application for flexible operation case

The maximal power capacity of the heating system, as well as the surface and the core temperatures are applied as constraints. To preclude the potential for misrepresenting system capabilities and to align with actual performance metrics, the heat pump's thermal output capacity was deliberately constrained to its true operational limit of 57 kW. This measure ensures that the simulated energy consumption aligns with realistic operational conditions and does not inadvertently optimize the system's performance based on unrealistically high-capacity figures, which could distort the assessment of building-grid interaction measures and the analysis of economic viability.

In employing control strategies for heating purposes, the surface temperature is maintained at a maximum of 24°C to ensure occupant comfort. The core temperature is intentionally set higher, within limits that preserve the structural integrity of the concrete and optimize the system's thermal efficiency. This differential in temperatures allows the stored heat to gradually permeate to the surface, providing a sustained release of warmth.

The decision-making process behind our rule-based control algorithm was guided by a multi-objective rationale, prioritizing cost reduction, energy efficiency and occupant comfort. The development of the algorithm involved an iterative process, where various input variables like energy prices, consumption patterns, and environmental conditions were analyzed.

Results

In the results section, we systematically analyze several key performance metrics of the building's operation during the week of December 5th to December 11th. The operation of the heat pump, which corresponds with price signals, is evaluated. Variations in surface temperatures are examined to assess the impact of the control strategy employed. The simulation results of heat flux density offer insights into the thermal loading and unloading cycles of the building's thermal mass. Indoor temperature data demonstrate the effectiveness of our control approach. Additionally, the battery's charging and discharging cycles are investigated, emphasizing the effectiveness of short-term load shifting strategies. Patterns of energy consumption shifted from the grid are delineated, and finally, the economic implications of these operational strategies are explored, underlining potential cost savings.

Heat pump operation

Figure 7 illustrates the temperature of the water supplied by the heat pump. It compares the BAU and FC scenarios, showing fluctuations in temperature across the monitored period. The BAU scenario operates within a narrower temperature range, suggesting a set temperature target that does not change with an external factor such as price signal. FC scenario allows for more variability in temperature, which indicates adaptive strategies to optimize cost optimization based on price signals and demand response requirements.

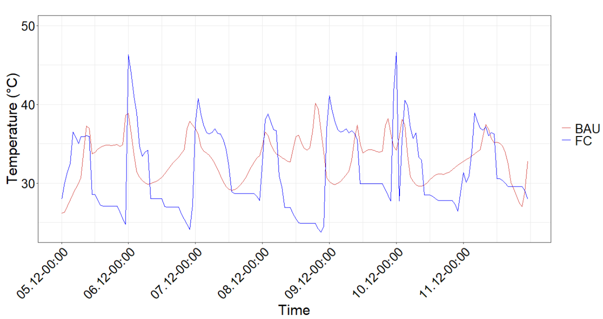

Figure 7 Heat pump supply water temperature

The analysis reveals a distinct operational adjustment in the FC scenario during periods of low electricity prices. For instance, on December 6th at 00:00, the supply temperature in the FC scenario is approximately 10°C higher compared to the BAU scenario, suggesting anticipatory thermal storage in anticipation of higher prices. Conversely, at around 23:00 on the same day, the supply temperature in the FC scenario decreases by an estimated 15°C below the BAU level in response to a spike in electricity prices.

The electrical power demand of the heat pump is shown in Figure 8. Depending on the outdoor temperature and load variations, the COP of the heat pump was found to range between 3 and 5. For the power demand in the BAU scenario, the consumption appears relatively steady, with predictable peaks that could correspond to regular daily usage patterns and fixed setpoint temperatures. Contrastingly, the FC scenario demonstrates periods where the power demand sharply decreases below BAU levels, indicating adaptive energy use in response to variable pricing. These drops correspond to periods where the system load shifts and battery discharge to reduce power usage from grid when electricity prices are higher. Notably, on December 6th from 10:00 am onwards, the FC scenario registers minimal to no power demand as a strategic response to the high or typical electricity price brackets, showcasing the implementation of a demand-side management strategy. Conversely, at 00:00 on December 6th, there is a significant surge in the FC scenario's power demand, which is twice that of BAU, corresponding to the elevated supply temperature.

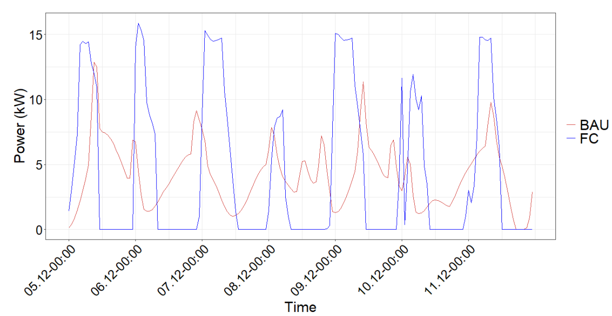

Figure 8 Heat pump power demand

Surface temperature variations

The implications of the rule-based control strategy on the surface temperature profiles across the four different office orientations —Southeast (SE), Northwest (NW), Southwest (SW), and Northeast (NE) are observed. In all offices, there are noticeable differences between BAU and FC temperature profiles, which suggests that the FC operations are affecting the surface temperatures within the building (Figure 9).

The FC curves appear to show greater fluctuations compared to the BAU curves, implying more dynamic control in response to price signals. If the price of electricity is lower, the system stores thermal energy -heating up- or using less energy -allowing temperatures to drop-. Conversely, if the price is high, the system may reduce energy use, leading to a drop in temperatures, or release stored thermal energy. The patterns appear relatively consistent across the four offices, which indicates a centralized control strategy for temperature management that affects all areas uniformly. In the BAU operation, temperatures exhibit fluctuations within a range of approximately 22.5°C to 24°C.

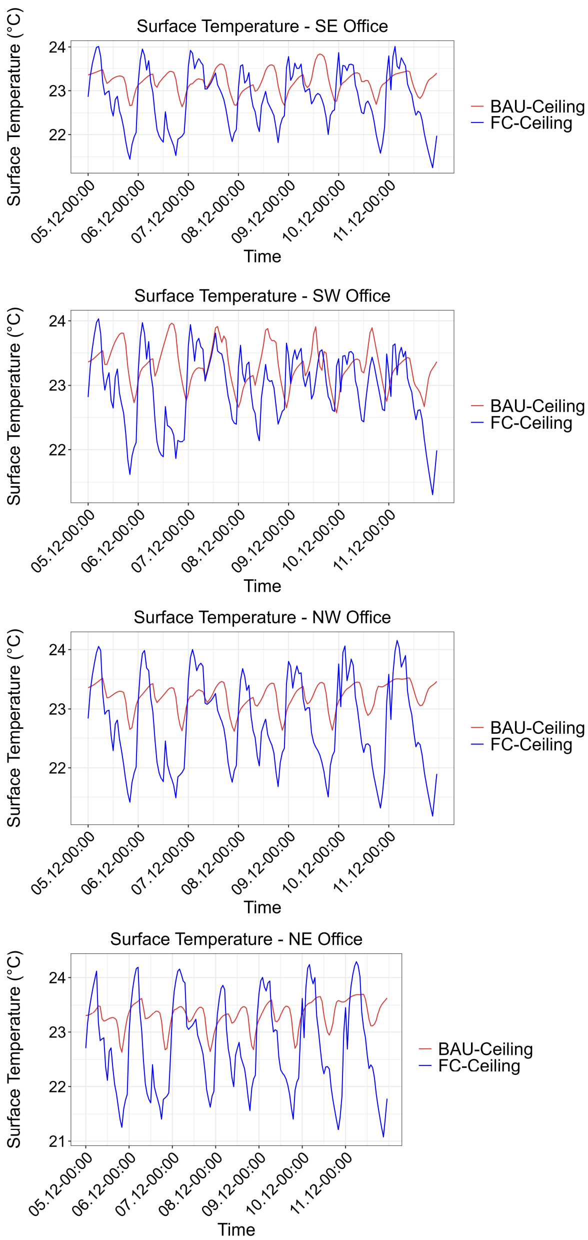

Figure 9 Surface temperature variations

However, in the FC operation, the lower boundary has notably reduced to 21°C, and surface temperatures demonstrate a broader oscillation, spanning a 3°C range. At 06:00 pm on 06.12, the ceiling temperature in the BAU scenario registers at approximately 23.5°C, while in the FC scenario, it measures around 22°C. This reflects a notable 1.5°C decrease attributable to the flexible case strategy.

Heat flux density

Figure 10 displays a cyclical pattern reflecting flux variations influenced by the building´s operational schedules and the dynamic nature of internal heat gains and losses. The FC scenario exhibits higher peaks and lower troughs in heat flux compared to the BAU scenario. This suggests that in the FC scenario, the building's thermal mass is strategically utilized to absorb heat during times when energy prices are low, storing it for later use. During times when energy prices are high, the building then minimizes energy consumption and relies on the stored heat, reducing operational costs.

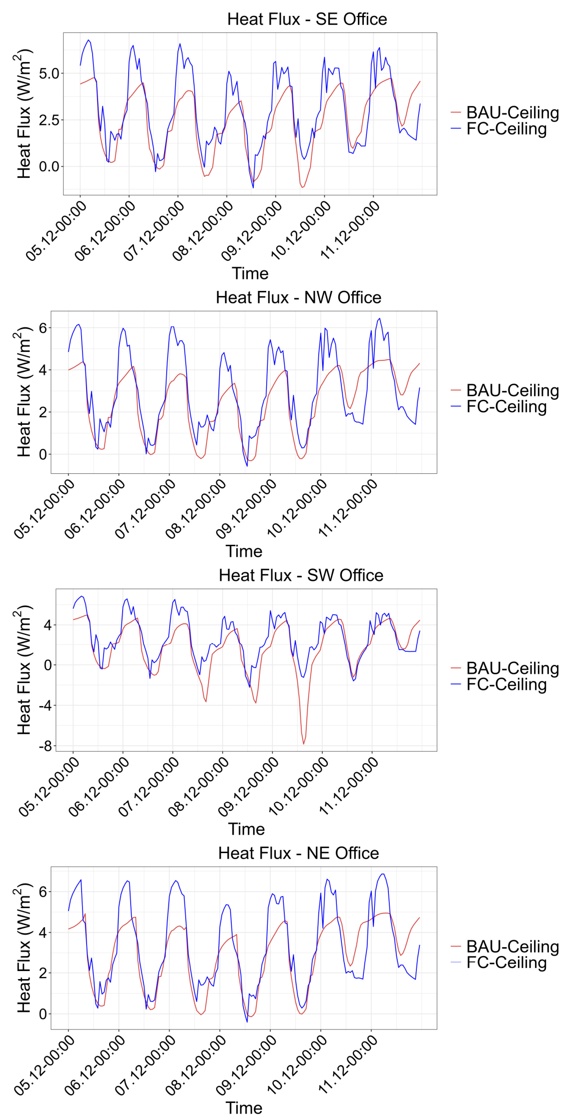

Figure 10 Heat flux variations

The BAU scenario, in contrast, shows a more uniform heat flux, indicating a consistent but less economically responsive use of energy. Across all four offices, the FC strategy demonstrates a coherent approach to managing heat transfer to achieve cost efficiency.

In the heating phase, TABS systems engage in thermal loading, capturing and storing heat within the building's mass. This stored energy is strategically released during thermal unloading to provide warmth, thus minimizing the need for active heating. The thermal energy storage behavior under BAU (Table 1) and FC strategies (Table 2 and Table 3) for the 5th of December was observed for relevant office zones in the building, indicating distinct operational profiles.

Table 1 The loading cycle in NW and NE- FC scenario

	SE		**NW**	
Loading (kWh)	3.8	0.6	3.4	0.4
Loading period (hour)	01:00-08:00	16:00-20:00	01:00-08:00	17:00-20:00
Unloading period (hour)	08:00-16:00	20:00-21:00	08:00-17:00	20:00-21:00
	SW		**NE**	
Loading (kWh)	2.7	0.9	4	1.5
Loading period (hour)	01:00-08:00	18:00-00:00	01:00-09:00	18:00-00:00
Unloading period (hour)	08:00-16:00	-	09:00-17:00	-

The analysis pertains to the ceiling thermal loading and unloading cycles. Under BAU conditions, the SE zone underwent a thermal loading of 3.8 kWh, executed during the early morning hours (01:00-08:00), followed by an 8-hour unloading period (08:00-16:00). The FC strategy modified the loading to 3.4 kWh, distributed across three intervals (01:00-05:00, 11:00-12:00, 18:00-20:00), thereby demonstrating a segmented approach synchronized with periods of lower energy tariffs and thermal comfort optimization. Correspondingly, the thermal unloading was partitioned into three segments (05:00-11:00, 12:00-15:00, 20:00-21:00), indicative of a refined strategy to modulate indoor conditions. The discernible pattern established for the SE zone provides a framework to interpret the thermal loading and unloading behaviors in the remaining zones. While the specific values and timings differ, the underlying principles observed in the SE analysis can be extrapolated.

Table 2 The loading cycle in SE and SW - FC scenario

	SE			
Loading (kWh)	3.4	0.5	0.3	0.5
Loading period (hour)	01:00-05:00	11:00-12:00	15:00-16:00	18:00-20:00
Unloading period (hour)	05:00-11:00	12:00-15:00	16:00-18:00	20:00-21:00
	SW			
Loading (kWh)	2.3	0.4	0.2	0.2
Loading period (hour)	01:00-05:00	11:00-12:00	15:00-16:00	17:00-19:00
Unloading period (hour)	05:00-11:00	12:00-15:00	16:00-17:00	19:00-21:00

The FC strategy's inclination towards segmented operations is evident, likely mirroring the price signal-driven approach that governs the FC system's engagement with the energy market and thermal comfort requirements.

Table 3 The loading cycle in NW and NE- FC scenario

	NW		
Loading (kWh)	3.5	0.5	0.4
Loading period (hour)	01:00-06:00	11:00-12:00	18:00-20:00
Unloading period (hour)	06:00-11:00	12:00-15:00	20:00-21:00
	NE		
Loading (kWh)	4	0.4	0.2
Loading period (hour)	01:00-07:00	11:00-12:00	17:00-20:00
Unloading period (hour)	07:00-11:00	12:00-15:00	20:00-21:00

Indoor temperature variations

In this section, the operative temperatures of four zones are compared between the BAU and FC. Figure 11 represents the temperature variations, aligning with the response of the heat pump operation to the price signal. Under BAU conditions, operative temperatures commence their ascent at approximately 08:00, culminating in afternoon peaks. Notably, the temperature within the SE office peaks between 22°C and 24°C, an outcome attributable to increased solar gains given its orientation. In contrast, the FC scenario sees operative temperatures spanning from 20.5°C to 23°C, with the occurrence of multiple peaks throughout the day. These peaks correlate with the timing of thermal loading and unloading, as well as variations in surface temperatures.

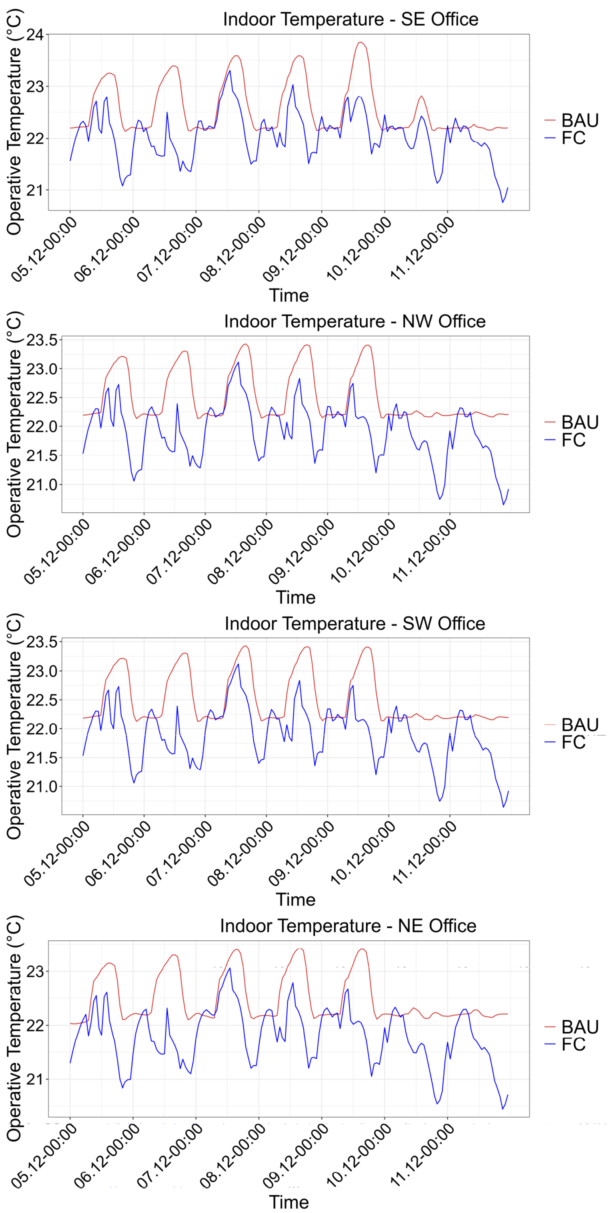

Figure 11 Operative temperature variations

The extended duration of loading/unloading cycles under FC operations induces more pronounced temperature transitions; however, these transitions are gradual enough that occupants are unlikely to perceive them as discomfort.

Battery charging /discharging cycle

Figure 12 depicts the battery charging and discharging patterns under BAU and FC scenarios. In the BAU scenario, battery usage is optimized for self-consumption: excess PV-generated electricity is used to meet the building's immediate electrical demands before charging the battery. The low PV generation in winter results in minimal battery charging from this source. There is no strategy in place for charging from the grid. The pattern of occasional and minor charging and discharging events suggests that the battery system mainly operates on electricity from PV sources. This infrequent battery utilization indicates a consistent and direct use of PV generation for real-time energy requirements.

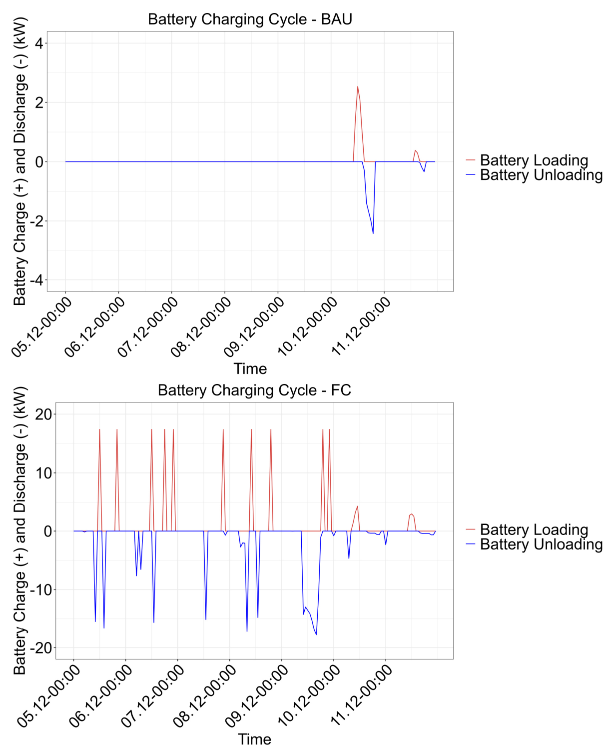

Figure 12 Battery charging /discharging cycle

In stark contrast, the FC scenario is characterized by a significantly more active battery cycle, with regular and notable charging and discharging. This pattern suggests a strategic and adaptive energy management approach. Here, the system not only responds to the PV generation but also actively manages the battery storage in anticipation of fluctuating grid electricity prices, irrespective of the lower winter PV output. The FC system's responsive charging strategy leverages periods of lower prices or excess PV generation, storing energy that can be used during peak price periods or when PV generation is insufficient. Such an approach indicates a nuanced understanding of energy management that balances self-generated renewable energy with the dynamics of grid electricity costs, maximizing economic efficiency.

Figure 13 indicates that the building consumes power from the grid but seldom feeds power back as shown by the lack of significant downward peaks. This unidirectional interaction suggests that the building under the BAU scenario predominantly relies on the grid for its energy needs, without offering flexibility services to the grid. The FC scenario shows a more complex pattern of interaction with the grid. There are numerous instances where the building consumes power from the grid and periods where it feeds energy back into the grid. This bidirectional interaction is characteristic of a more integrated and responsive energy management system that not only consumes energy from the grid but also leverages the stored energy in the batteries to supply the grid, reflecting active participation in demand response and energy balancing.

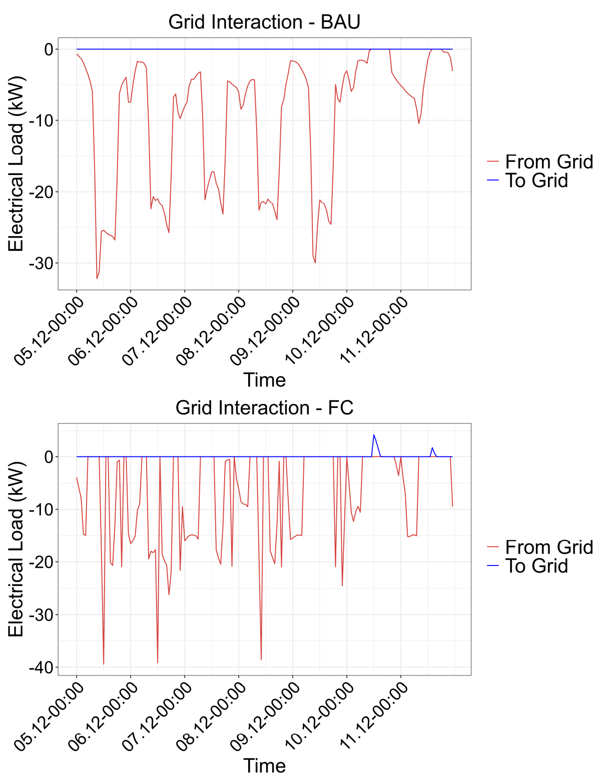

Figure 13 Building-grid interaction

Short-term load shifting

Figure 14 shows the difference in total power demand of all actors in the building except electrical storage between the BAU scenario and the FC scenario over time, with an hourly resolution. The data represents a period of one week between the 5th of December to 11th of December. When the bars are above the zero line, this indicates that the FC scenario demands more power than the BAU scenario during that hour. This occurs due to the FC scenario responding to lower price signals and thus consuming more energy to heat the building to mitigate costs later. Vice versa, when the bars are below the zero line, the FC scenario uses less power than the BAU scenario. This corresponds to periods when the FC scenario is capitalizing on high energy prices or employing energy-saving measures that were not used in the BAU scenario. The taller the bar, the greater the difference in power demand between the FC and BAU scenarios during that hour.

The range of values spans from around -10 kW to just above 15 kW. This indicates that the maximum additional power consumption in the FC scenario compared to BAU is about 15 kW, and the maximum savings are about 10 kW. In the FC operational scenario, an overall increase in demand of 77 kW has been observed for this representative week, which is consistent with the tendency for building-grid operations to amplify heating demand. This phenomenon often occurs as flexibility measures, such as load shifting, incentivize the use of heating systems at times when electricity is less expensive. Within this overall increase, the heat pump control strategy has specifically contributed approximately 35 kW.

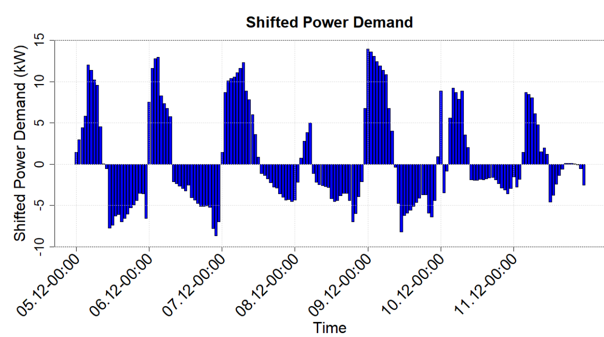

Figure 14 Shifted electrical energy demand of all building operations

Figure 15 represents the difference in energy consumption from the power grid between two scenarios over time, including the effect of electrical storage. The vertical axis shows consumption differences ranging from approximately -30 kWh to +20 kWh. This indicates significant variability, with the FC scenario sometimes consuming substantially more energy than BAU and at other times substantially less. The graph shows considerable volatility, with sharp increases and decreases in energy consumption differences. This suggests a dynamic energy management system in the

FC scenario, likely influenced by various factors such as price signals and storage charging/discharging cycles. The inclusion of electrical storage explains the differences between BAU and FC in Figure 13. Energy storage systems can absorb excess energy during periods of low demand and release energy during periods of high demand, smoothing overall consumption patterns. Under the FC scenario, a significant reduction of 400 kWh in energy consumption from power grid is achieved, underscoring the effectiveness of this operational strategy, particularly when battery storage is incorporated to optimize load shifting and harness charging when prices favorable.

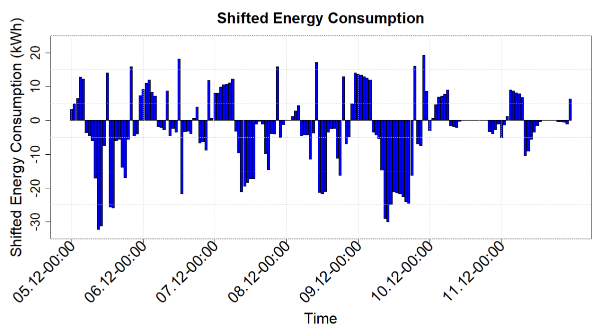

Figure 15 Shifted electrical energy consumption from power grid

Cost saving

Figure 16 illustrates the difference in cost between FC scenario and BAU scenario over the representative period. The cost differences range from approximately -15€ to +10€, with negative values indicating cost savings and positive values indicating additional costs compared to BAU.

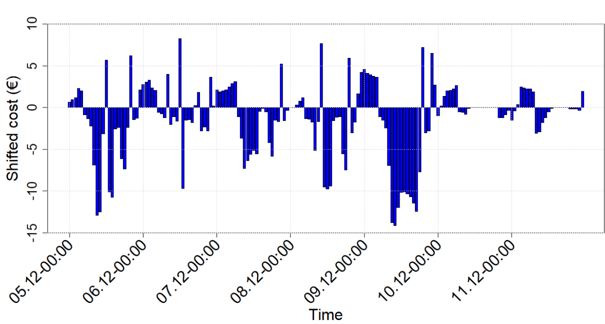

Figure 16 Shifted operational cost

The graph predominantly features negative values, suggesting that the FC scenario more frequently results in cost savings compared to the BAU scenario. There are fewer instances where the cost is higher than BAU, and these do not exceed +10€, suggesting that the FC scenario's cost increases are less severe than its savings. Similar to Figure 15, this cost graph also shows considerable volatility, which implies that the cost savings are not constant over time but fluctuate significantly. In the FC scenario, 220 euros are saved for the representative week, highlighting the economic benefits of this operational strategy.

Conclusion

This investigation into the operational dynamics of a building under Business-as-Usual (BAU) and Flexible Control (FC) scenarios has yielded significant insights into the complex interplay between building performance, energy management, and economic efficiency. The operative temperatures observed in the FC scenario demonstrated a sophisticated strategy of thermal loading and unloading, aligning with the heat pump's operational response to the variable pricing signals. The resulting temperature profiles indicate that, despite the multiple thermal peaks resulting from strategic thermal storage and release cycles, the FC scenario maintains comfort within acceptable operative temperature ranges.

In the realm of energy storage, the FC scenario's proactive battery charging and discharging pattern starkly contrasts with the BAU scenario's passive approach. This active energy management strategy, which takes advantage of lower grid prices and surplus photovoltaic generation, underscores the potential of battery storage systems to enhance both economic savings and energy resilience. The grid interaction patterns indicate that the building's energy exchange under the FC scenario transitions from unidirectional to bidirectional. This shift not only optimizes energy costs through demand response participation but also contributes positively to grid stability by offering flexibility services.

Regarding short-term load shifting, the FC scenario reveals an adeptness in adjusting power demand to price signals, a strategy that underscores the significance of load shifting in operational cost reduction. The heat pump's control strategy, instrumental in this approach, maximizes the use of cheaper off-peak electricity and minimizes dependency on higher-cost grid energy during peak periods.

The study's focus on thermal loading and unloading dynamics, as well as the regulation of heat flux within the building envelope, has further illustrated the nuanced control the FC scenario exerts over the internal climate. By modulating the heat pump operation in conjunction with the inherent thermal inertia of the building's structure, the FC scenario optimizes thermal comfort and energy efficiency.

Finally, the economic analysis of the FC scenario reveals a compelling narrative of cost savings, with a significant reduction in energy expenses over the analysis period. The saving of 220 euros during a representative week exemplifies the financial viability of intelligent energy management systems that encompass advanced control of thermal loading, unloading, and heat flux alongside strategic energy storage use.

In conclusion, the evidence from this study supports the premise that adaptive, intelligent building controls and energy management strategies, such as those embodied in the FC scenario, are pivotal in enhancing the operational performance of buildings. By effectively managing thermal energy flows, optimizing battery storage, and interacting dynamically with the energy grid, such systems promise significant improvements in both economic and environmental performance for the built environment. The implications of this research extend beyond individual buildings, offering scalable strategies that can contribute to the broader goals of sustainable urban development and smart grid integration.

In future research, exploring advanced control strategies such as Model Predictive Control (MPC) presents a promising avenue. MPC, known for its ability to forecast and optimize building performance by considering future conditions, could significantly enhance energy efficiency and operational cost savings. This approach, combined with AI and machine learning algorithms, could provide a more sophisticated, predictive optimization of energy systems. Additionally, integrating IoT and smart sensors would enable finer control and real-time data utilization. The exploration of renewable energy integration and advanced demand response strategies also aligns with the evolving smart grid ecosystem. These advancements would not only elevate building-grid interactions but also contribute to sustainable energy management solutions.

Acknowledgment

The authors would like to express their gratitude to the International Energy Agency's Energy in Buildings and Communities Programme Annex 82, for supporting the research work presented in this article. Additionally, we extend our thanks to the Equal Opportunities Officer at the University of Wuppertal for providing the funding that enabled our participation in this conference.

References

Andy Staff (2022). "Goblet Lavandier & Associés Ingénieurs-Conseils S.A. - Photo".

Arteconi, A., D. Costola, P. Hoes and J. Hensen (2014). "Analysis of control strategies for thermally activated building systems under demand side management mechanisms". Energy and Buildings 80: 384–393. DOI: 10.1016/j.enbuild.2014.05.053.

B.W. Olesen (2007). "Operation and Control of Activated Slab Heating and Cooling Systems". Chen, Q., N. Li and W. Feng (2021). "Model predictive control optimization for rapid response and energy efficiency based on the state-space model of a radiant floor heating system". Energy and Buildings 238: 110832. DOI: 10.1016/j.enbuild.2021.110832.

Cho, S.-H. and M. Zaheer-uddin (1999). "An experimental study of multiple parameter switching control for radiant floor heating systems". Energy 24(5): 433–444. DOI: 10.1016/S0360-5442(98)00101-7.

ENTSO-E Transparency Platform (Dec-2022, Dec-2022). "Day-ahead Prices". Retrieved Dec-2022, from https://transparency.entsoe.eu/dashboard/show.

Feng, J., F. Chuang, F. Borrelli and F. Bauman (2015). "Model predictive control of radiant slab systems with evaporative cooling sources". Energy and Buildings 87: 199–210. DOI: 10.1016/j.enbuild.2014.11.037.

Gwerder, M., B. Lehmann, J. Tödtli, V. Dorer and F. Renggli (2008). "Control of thermally-activated building systems (TABS)". Applied Energy 85(7): 565–581. DOI: 10.1016/j.apenergy.2007.08.001.

Hanova, J. and H. Dowlatabadi (2007). "Strategic GHG reduction through the use of ground source heat pump technology". Environmental Research Letters 2(4): 44001. DOI: 10.1088/1748-9326/2/4/044001.

IDA-ICE (2023). "Equa Simulation AB - IDA indoor climate and energy 4.8 - Simulation Software | EQUA". Retrieved 15-Aug-23, from https://www.equa.se/en.

Lee, C. K. (2011). "Effects of multiple ground layers on thermal response test analysis and ground-source heat pump simulation". Applied Energy 88(12): 4405–4410. DOI: 10.1016/j.apenergy.2011.05.023.

Lehmann, B., V. Dorer and M. Koschenz (2007). "Application range of thermally activated building systems tabs". Energy and Buildings 39(5): 593–598. DOI: 10.1016/j.enbuild.2006.09.009.

Li, R., A. J. Satchwell, D. Finn, T. H. Christensen, M. Kummert, J. Le Dréau, R. A. Lopes, H. Madsen, J. Salom, G. Henze and K. Wittchen (2022). "Ten questions concerning energy flexibility in buildings". Building and Environment 223: 109461. DOI: 10.1016/j.buildenv.2022.109461.

Li, Y., J. Wang, Y. Han, Q. Zhao, X. Fang and Z. Cao (2020). "Robust and opportunistic scheduling of district integrated natural gas and power system with high wind power penetration considering demand flexibility and compressed air energy storage". Journal of Cleaner Production 256: 120456. DOI: 10.1016/j.jclepro.2020.120456.

Lichtmess, M. (2018). "Objektbericht Goblet Lavandier & Associés".

Lim, J.-H., J.-H. Jo, Y.-Y. Kim, M.-S. Yeo and K.-W. Kim (2006). "Application of the control methods for radiant floor cooling system in residential buildings". Building and Environment 41(1): 60–73. DOI: 10.1016/j.buildenv.2005.01.019.

Reynders, G., T. Nuytten and D. Saelens (2013). "Potential of structural thermal mass for demand-side management in dwellings". Building and Environment 64: 187–199. DOI: 10.1016/j.buildenv.2013.03.010.

Rhee, K.-N. and K. W. Kim (2015). "A 50 year review of basic and applied research in radiant heating and cooling systems for the built environment". Building and Environment 91: 166–190. DOI: 10.1016/j.buildenv.2015.03.040.

Rhee, K.-N., B. W. Olesen and K. W. Kim (2017). "Ten questions about radiant heating and cooling systems". Building and Environment 112: 367–381. DOI: 10.1016/j.buildenv.2016.11.030.

Romaní, J., A. de Gracia and L. F. Cabeza (2016). "Simulation and control of thermally activated building systems (TABS)". Energy and Buildings 127: 22–42. DOI: 10.1016/j.enbuild.2016.05.057.

Salt, H. (1985). "Preliminary design considerations for a rockbed/floor space-heating system". Building and Environment 20(4): 221–231. DOI: 10.1016/0360-1323(85)90037-X.

Shin, M. S., K. N. Rhee, S. R. Ryu, M. S. Yeo and K. W. Kim (2015). "Design of radiant floor heating panel in view of floor surface temperatures". Building and Environment 92: 559–577. DOI: 10.1016/j.buildenv.2015.05.006.

Stackhouse, P. (2023). "NASA- Power - Data Access Viewer". Retrieved 10-11-2023, from https://power.larc.nasa.gov/data-access-viewer/.

Tian, Z. and J. A. Love (2009). "Energy performance optimization of radiant slab cooling using building simulation and field measurements". Energy and Buildings 41(3): 320–330. DOI: 10.1016/j.enbuild.2008.10.002.

Vivek, T., C. Rakesh, B. K, P. K and M. Arıcı (2023). "Indoor thermal comfort analysis of TABS with untreated natural ventilation in a warm and humid climate – An experimental study". Journal of the Taiwan Institute of Chemical Engineers 148: 104921. DOI: 10.1016/j.jtice.2023.104921.